INFLUENCE OF CELLULOSE NANOCRYSTALS ON THE MECHANICAL PROPERTIES AND CRYSTALLIZATION OF NYLON 6 COMPOSITES

Jankovic, N[1], Demir, E[2], Ayranci, C[2], and McDermott, M[1]*
[1] Department of Chemistry, University of Alberta, Edmonton, Canada
[2] Department of Mechanical Engineering, University of Alberta, Edmonton, Canada
* Corresponding author (mark.mcdermott@ualberta.ca)

Keywords: *cellulose nanocrystals, nylon 6, films*

ABSTRACT

The use of cellulose-based nanomaterials in the fabrication of advanced polymer composites is an ongoing target. Cellulose nanocrystals (CNC) have been widely used in composites as they give rise to large increases in elastic modulus at low loadings. Nylon 6 (or Polyamide 6) is one of the most commonly used polymers for the production of industrial fibres, ropes, and thin films. It has been shown to change crystal structure depending on the processing technique or the addition of fillers. In this study, spin coated CNC-Nylon 6 films and electrospun fibres were produced. The addition of CNC increased the elastic modulus of the composites up to 1 wt%; however, polymer crystallization was inhibited as seen using FTIR, DSC, and XRD. The thermal stability of the composites also decreased due to the earlier degradation of CNCs. This work provides an exciting route towards CNC reinforced composites for applications in film packaging and textiles.

1 INTRODUCTION

Interest in cellulose nanomaterials has expanded over the past few decades. The appeal in using a cellulose-based filler in composites is due to the biorenewability and biodegradability of the material itself as it is typically produced from byproducts from the forestry industry.[1] Specifically, cellulose nanocrystals (CNC) have been widely used in composites as they give rise to large increases in elastic modulus with very low loadings (<10 wt%).[1,2] The carbon and oxygen rich CNC nanoparticles can favourably interact with a polymer matrix *via* hydrogen bonding on the surface, and alongside the highly crystalline and stiff nature of CNCs, they have been shown to increase the mechanical, thermal, and conductive properties of numerous polymers.[1] The tensile strength along the length of CNC is around 7500-7700 MPa and the elastic modulus is around 120-143 GPa, which make CNC an excellent candidate for mechanical reinforcement.[3,4]

Many polymers have been reinforced with CNC with the goal of an increased mechanical response, such as polylactic acid (PLA) and polyethylenes (PE),[5,6] but only a handful have looked at polyamides. Nylon 6 (or Polyamide 6) is one of the most commonly used polyamides in the world. It is most commonly manufactured as fibres that are used in textiles or molded into parts for automotive vehicles.[7] Thus, researchers have looked into harnessing the reinforcing strength of CNC with the goal of product longevity and stronger materials. Most of the focus has been on industrially relevant melt-mixing approaches such as injection or compression molding.[8,9] However, CNC degrades at temperatures around 240°C which causes burning and discoloration of molded samples.[10] Additionally, achieving good dispersions of CNC in a polymer melt is difficult to control. Thus,

solvation of CNC prior to addition to a polymer, such as in electrospinning or solvent casting, can avoid degradation of the nanomaterial during processing and allow for good dispersions.[11]

Herein, this study elaborates on the characterization of CNC reinforced Nylon 6 films previously reported from our group.[12] An investigation into the effect of CNC on the mechanical properties of the composites is presented. Crystallinity plays a large role in the mechanical properties of the composite, thus FTIR, DSC, and XRD are used to study the crystallinity of the samples. The thermal stability of the composites using TGA and DTG is also reported. Finally, preliminary work into the electrospinning of CNC-Nylon 6 nanofibres *via* electrospinning is presented.

2   MATERIALS AND METHODS

2.1 *Materials*

Nylon 6 pellets (CAS No. 25038-54-4) were purchased from MilliporeSigma Canada (Oakville, ON, CA). Spray-dried sulfate half-ester Na-form cellulose nanocrystals (CNC) were purchased from Celluforce (Montreal, QC, CA). BD PrecisionGlide needles (20 g x 1 (0.9 mm x 25 mm)) and 3 mL luer lock BD syringes (I.D. = 8.56 mm) were purchased from MilliporeSigma Canada (Oakville, ON, CA). The needle tips were sanded down using a Dremel rotary sander with a 180-grit sanding disc to obtain blunt-end needles (Mount Prospect, IL, USA). Acros Organic Formic acid (FA, 98%+) was purchased from Fisher Scientific Canada.

2.2 *Preparation of CNC-Nylon 6 Solutions & Production of Thin Films and Electrospun Mats*

Electrospinning solutions of 20 wt/v% (total solids/solvent) were prepared by adding cellulose nanocrystals to formic acid (1 wt/wt% CNC/Nylon 6) and bath sonicating for 30 minutes. Nylon 6 pellets were added to the solutions (100 and 99 wt/wt% Nylon 6/CNC) while magnetically stirring. The solutions were left to stir overnight at ambient conditions until all the pellets were dissolved. Each solution was vortexed then sonicated for 5 minutes prior to composite production.

The spin coated films were prepared using a previously reported procedure by Osorio *et al.*[12] Briefly, a syringe was used to deposit 2 mL of solution onto cleaned microscope slides then spin coated at: 300 rpm for 15s, then 1000rpm for 60s, then 1300rpm for 15s. Electrospun fibre mats were collected on a 20cm x 20cm stainless steel plate that was covered with aluminum foil. A single 3mL syringe with a blunt-tip needle was used. Electrospinning was performed with a constant flow rate of 2 μL/min, a constant voltage of 21 kV, and a working distance (tip of syringe needle-to-collector distance) of 10 cm. Electrospinning time was 3 hours for each sample and done at ambient conditions (RH ~ 37% and T ~ 21˚).

2.3 *Characterization*

Scanning electron microscopy (SEM) images were taken using a Zeiss Sigma (Gemie) field emission scanning electron microscope. Electrospun samples were kept on the aluminum foil and cut into 1cm x 1cm squares then placed onto SEM stubs using carbon tape. All samples were imaged using an EHT of 3.00 kV and using the SE2 Everhart-Thornley detector. Image analysis was completed using the ImageJ software. Fourier transform infrared (FT-IR) analysis was completed using a Thermo Nicolet 8700 FTIR Spectrometer. A freestanding sample was cut from each composite and placed in the pathlength of the laser. All spectra were collected from 4000 to 650 cm^{-1} at 128 sample scans a resolution of 4.000. Differential scanning calorimetry (DSC) was completed using a TA Instruments DSC-Q1000. Samples (4-5mg) were placed in a hermetic aluminum DSC pan, then heated from 25˚C to 250˚C at a heating rate of 10˚C/min and under nitrogen. In the degree of crystallinity calculations, a value of 230 J/g for ΔH_f^{100} of Nylon 6 was used. Data was processed using the TA Universal Analysis software. Thermogravimetric analysis (TGA) was competed using a TA Instruments Discovery TGA. Samples (4-5mg) were placed in a platinum sample

holder, then heated from 25°C to 500°C at heating rate of 10°C/min and under nitrogen. Data was processed using the TA Universal Analysis software. X-Ray diffraction (XRD) analysis was completed using a Rigaku Ultima IV XRD. It was equipped with a Cu x-ray target, with operating voltage of 40 kV and 44 mA. The parallel beam was used at a scan axis of 2theta with glancing angle omega at 0.5°. Scan mode was continuous, sampling width was 0.05° with a range from 8° to 38°, and a scan speed of 2°/min was used. The divergence slit was 0.1°. Data was processed using Jade 9.0 with ICDD database 2010. Mechanical tests were performed using a TA Instruments ElectroForce 3200 uniaxial testing machine (10 N max. capacity load cell). Test strips were prepared by cutting with a rotary cutter to obtain sample dimensions of 10 mm x 75 mm and peeling the samples from their respective substrates. All samples were stored in a desiccator for at least 12 hours to remove excess moisture and residual solvent. The tensile tester instrument has grips that hold 25 mm of the test strip, so gauge length was set to 50 mm between the grips. A C-shaped frame made from paper was used to hold the samples in the grips to prevent sliding of and reduce stress concentration on the samples during testing. All samples were placed between the grips in a way where the alignment direction of fibres was parallel to the testing direction. All tests were performed at ambient conditions. The strain rate was set at 0.1 mm/mm•min (5mm/min). The results were averaged over 5 measurements according to the ASTM D882-12 standard.[13]

3   RESULTS AND DISCUSSION

Spin coating was chosen as the initial processing method as it produces uniform freestanding films that can be easily manipulated for tensile testing. Furthermore, the solution processing of the composite allows for enhanced CNC dispersion within the Nylon 6 matrix, as discussed in Section 1. Thus, freestanding CNC-Nylon 6 thin films were produced at loadings of 0, 1, 2.5, and 5 wt% CNC and spin coated from formic acid. The addition of CNC to Nylon 6 was found to decrease the transparency of the films and increase the film thickness, as shown in Figure 1. The neat Nylon 6 films were translucent but became opaque with 2.5 wt% and 5 wt% CNC, implying that CNC was no longer fully dispersed in-solution at the higher loadings.[14] The increase in opacity of the films is similar to what Sucharitpong *et al.* observed in solvent cast CNC-Nylon 6 films.[14] Film thickness doubled with the addition of 5 wt% CNC when compared to the neat Nylon 6 films and the films were also more fragile when handling with increased loading.[12]
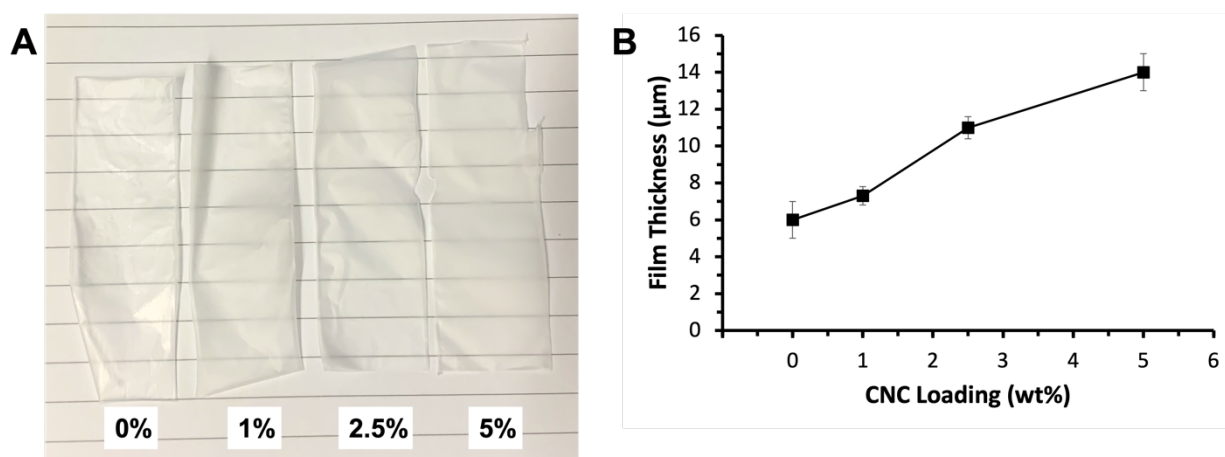

Figure 1. (A) Photographs of the thin films produced at CNC loadings of 0-5 wt% and (B) the corresponding thickness of the films at each CNC loading.

The dispersion quality of CNC within the films was visualized using TEM, as shown in Figure 2A and 2B. The neat polymer film in Fig. 2A is free of any particles. Sonication of the solutions is expected to allow for improved dispersion of individual CNC particles within the Nylon 6 matrix, thus, the image of the 5 wt% CNC film in Fig. 2B shows well-dispersed CNCs within the film. The size and shape of the dark fibrils seen in Fig. 2B are consistent with those of CNC.[15] When visualized under SEM in Fig. 2C and 2D, the morphology of the films shows the appearance of spherulite structures. Spherulites form when a crystalline polymer is cooled due to the radial stacking of the polymer chains around a crystal centre.[16] In the neat Nylon 6 film, the spherulites appear to be small and pack close together. In the 5 wt% CNC film, there appears to be less of the spherulite structures conducive to the inhibition of polymer crystallization due to the presence of a high CNC content.
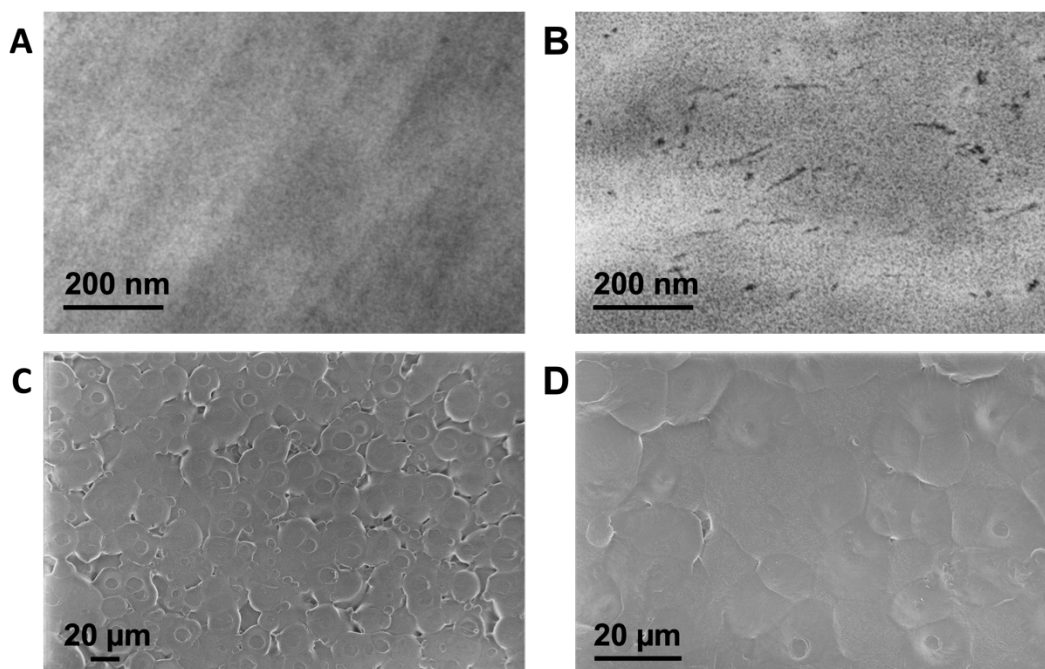

Figure 2. TEM images of (A) neat Nylon 6 film and (B) 5 wt% CNC film, and SEM images of (C) neat Nylon 6 film and (D) 5 wt% CNC film.

After confirmation of the presence of CNC, tensile tests were performed on the film samples. Analysis of the stress-strain curves are depicted in Figure 3, which show the values for Young's modulus (YM) (in blue) and ultimate tensile strength (UTS) (in red).[12] The neat Nylon 6 films exhibit a YM of 2.02 ± 0.06 GPa which is comparable to previous studies.[9,17,18] The Young's modulus increased by 49% after the addition of 1 wt% CNC, then decreased to similar values as the neat polymer for both 2.5 and 5 wt% CNC. The UTS showed a similar trend, with a value of 45 ± 4 MPa for neat Nylon 6 and an increase by 62% for 1 wt% CNC. There was also a decrease in UTS for 2.5 and 5 wt% CNC. The findings here are consistent with other studies that show a maximum in mechanical properties of CNC-Nylon composites at around 1 wt% CNC.[9,12,14]
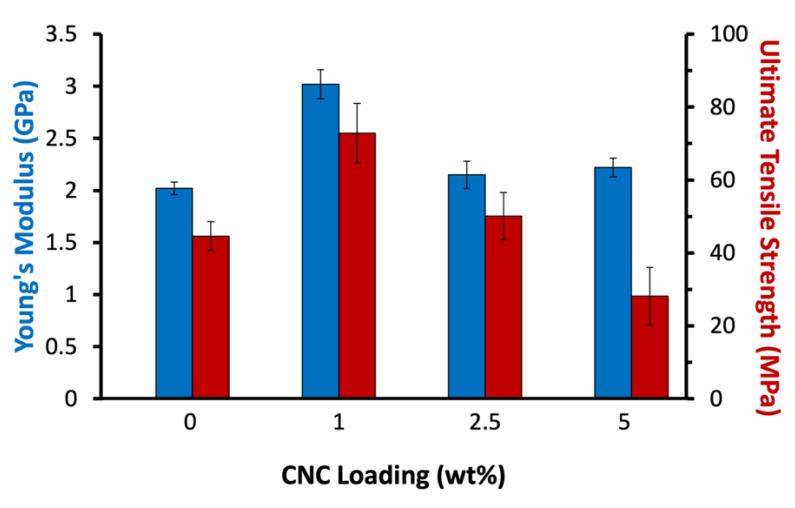
Figure 3. Young's modulus (blue) and ultimate tensile strength (red) results for the CNC-Nylon 6 films at 0, 1, 2.5, and 5 wt% CNC loadings.

To gain a better understanding of the influence of CNC in the films, the chemical composition of the films was investigated using FTIR, as presented in Figure 4. There is the presence of predicted Nylon 6 bands at 1169 cm^{-1}, 1123 cm^{-1}, and 1069 cm^{-1} as well as the appearance and increase of the glucose C2, C3, and C6 C-O stretching vibrations at 1116 cm^{-1}, 1062 cm^{-1}, and 1035 cm^{-1}, respectively, which further confirms the presence of CNC in the composites.[15] In addition to chemical composition, the FTIR spectra also provide insight into the crystalline microstructure of Nylon 6. The band at 972 cm^{-1} is attributed to the CONH in-plane stretching of the γ allomorph of Nylon 6 and the bands at 959 and 929 cm^{-1} are attributed to the CONH in-plane stretching of the α crystal allomorph of Nylon 6.[19,20] The α allomorph is the most stable form as it is a result of the extended planar conformation of the polyamide chains, whereas the γ form is the less stable form as it is the result of twisted chains.[21,22] The presence of the two bands at 959 and 929 cm^{-1} suggest that the spin-coated films mainly crystallize in the α form thus any changes in crystallization in the γ form must be due to CNC. The peak at 972 cm^{-1} is very weak suggesting that there is some crystallization of the polymer in the γ form due to CNC.[12]
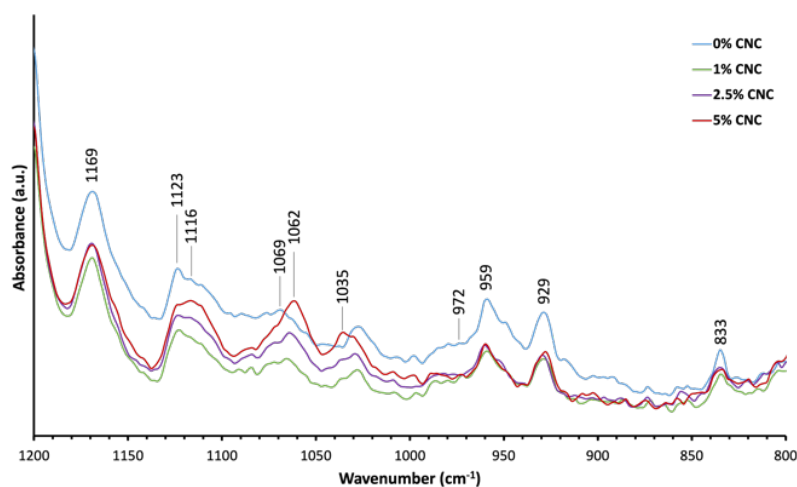

Figure 4. FTIR analysis of the spin-coated CNC-Nylon 6 films.

Further investigation into the effect of CNC on the crystalline behaviour of Nylon 6 was performed using DSC, as shown in Figure 5A.[12] The Nylon 6 α allomorph peak at 221˚C appears to dictate the crystallization temperature, however, there is a small shoulder at 206˚C attributed to the γ allomorph peak. Consistent with the data from FTIR, the DSC data shows that films preferentially crystallize in the α form.[23]

The degree of crystallinity (χ_C) of each composite was calculated from the DSC results using Equation 1,

$$\chi_C = \frac{\Delta H_f}{(1-\phi)\cdot \Delta H_f^{100}} \cdot 100\% \tag{1}$$

where ΔH_f is the heat of fusion of the composite, ϕ is the weight fraction of CNC, and ΔH_f^{100} is the heat of fusion of fully crystalline Nylon 6 (230 J/g).[24] The degree of crystallinity did not change with the addition of CNC, with values of 29.1% for the Nylon 6 pellet, 28.3% for 0 wt%, 27.8% for 1 wt%, 28.1% for 2.5 wt%, and 28.5% for 5 wt%.

Finally, TGA and DTG was used to investigate the thermal properties of the films. The TGA curves in Figure 5B show a small 2% decrease in weight loss at temperatures below 100˚C which is attributed to water loss due to absorbed water by both CNC and Nylon 6. The onset temperature (T_O) significantly decreased with the addition of CNC – from 421˚C for 0 wt% CNC to 409˚C for 5 wt% CNC – due to the earlier degradation of CNCs at temperatures around 200-300˚C.[25]. After 450˚C, there is a small remaining mass that is greater with higher CNC loadings due to the residual char leftover from CNC over after degradation.[25] In the DTG curves in Figure 5C, the first derivative peak temperature (T_P) also did not change with the addition of CNC, with values of 453˚C for 0 wt% CNC to 455˚C for 5 wt% CNC. Overall, the thermal stability of the composite decreased slightly with the addition of CNC due to the earlier decomposition of CNCs.
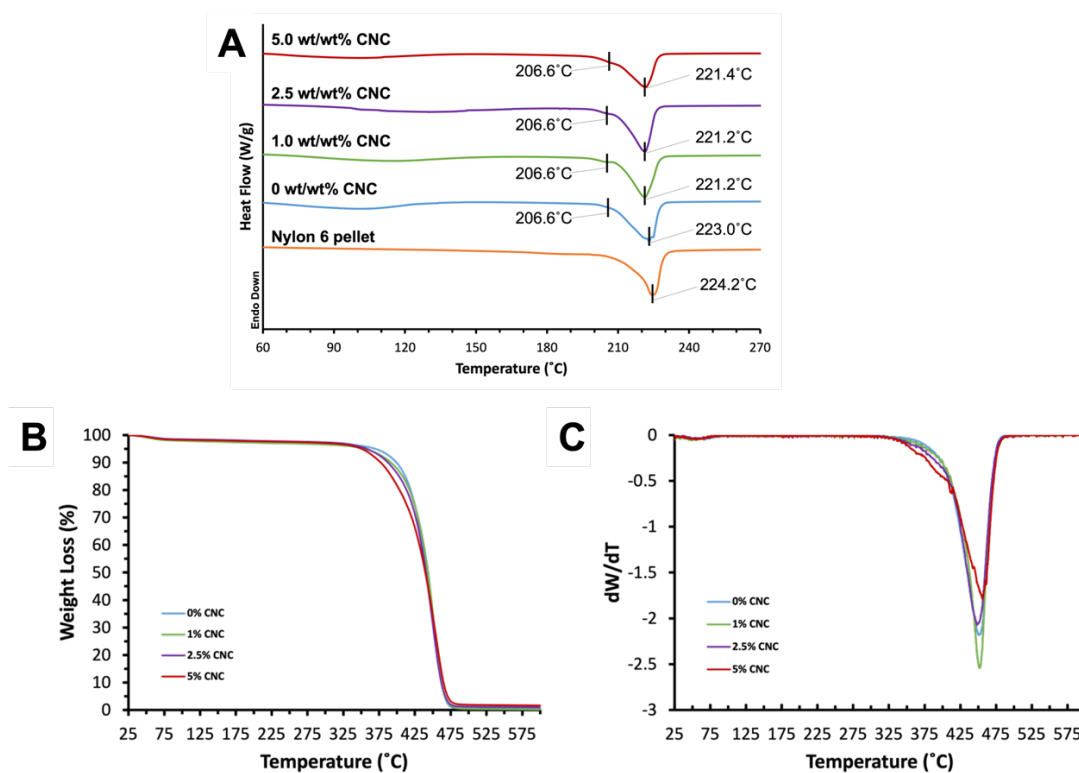

Figure 5. A) DSC, B) TGA, and C) DTG analysis of CNC-Nylon 6 films.

Upon seeing the significant increase in mechanical properties of the spin coated CNC-Nylon 6 films, electrospinning was used to produced composite nanofibres. Electrospinning is a quick and facile method to produce polymer fibres with diameters in the nano- to micro-meters.[26] A polymer is dissolved in a compatible solvent and this solution is loaded into a syringe. An applied voltage creates an electric field that overcomes the surface tension of the polymer solution which causes the solution to continuously discharge from the needle, forming a Taylor cone.[27,28] A jet is ejected from the tip of the Taylor cone followed by a straight stable and an instable region that resembles a whipping motion.[27] During the whipping motion, the solvent evaporates and the solidified polymer is collected onto a grounded collector as thin fibres orient randomly onto the substrate. The morphology of the resultant fibres is dependent on the processing and solution parameters, which include the flow rate, applied voltage, needle-to-collector distance, and type of collector, and viscosity, concentration, and conductivity of the polymer solution.[28-30]

Nanofibres of CNC and Nylon 6 were produced at the same loadings at the films. The SEM images of the fibres in Figure 6 show that they are smooth, long, and nanometer-sized in diameter. Average fibre diameter does not differ significantly between loadings, with average values of 129 ± 28 nm for 0 wt% CNC, 121 ± 21 nm for 1 wt% CNC, 123 ± 27 nm for 2.5 wt% CNC, and 111 ± 26 nm for 5 wt% CNC. There are a few ultra-fine secondary "spider-web" fibres seen in all samples, which form due to the ionization of the amide groups of Nylon 6 in formic acid under the high voltage applied during electrospinning.[31] The mechanical and chemical characterization of the fibres, including the alignment of the fibres within a fibre mat, will be the topic of future studies.
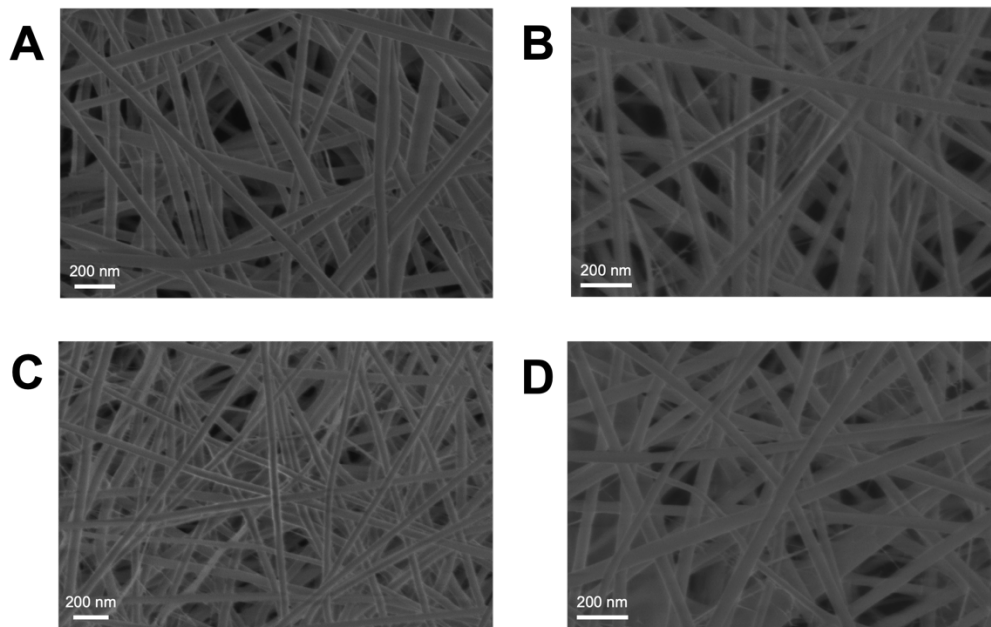

Figure 6. SEM images of the CNC-Nylon 6 electrospun fibre mats at (A) 0 wt%, (B) 1 wt%, (C) 2.5 wt%, and (D) 5 wt% CNC.

4 CONCLUSION

In this study, CNC reinforced Nylon 6 composite spin coated films and electrospun nanofibres were produced. The addition of CNC increased the mechanical properties of the films, including a 49% and 62% increase in YM and UTS, respectively, after the addition of 1 wt% CNC. There was no significant change in mechanical

properties of the higher loadings when compared to neat Nylon 6. SEM, FTIR, and DSC showed that the films predominately crystallized in the α crystal allomorph in Nylon 6 and that CNC induced the transition to the unstable γ form. However, the addition of the stiff and strong CNC nanoparticles appeared to overcome any decrease in mechanical properties solely due to a change in the crystalline structure of the polymer. Finally, the thermal stability of the polymer also decreased with the addition of CNC. Preliminary data for the electrospinning of CNC-Nylon 6 nanofibres was presented. Uniform fibres were produced as evidenced by SEM, and further characterization will be the topic of future studies. The work presented here provides an exciting route towards stronger fibres for textile applications, such as CNC reinforced ropes, yarns, and fabrics.

5 REFERENCES

[1]   A. Dufresne. "Cellulose nanomaterials as green nanoreinforcements for polymer nanocomposites". *Philos Trans A Math Phys Eng Sci,* Vol. 376, No. 2112, 2018.

[2]   D. Liu, G. Sui and Y. Dong, "5 - electrospun polymeric composite nanofibers with cellulose nanocrystals and their applications," in *Electrospun polymers and composites*, Y. Dong, A. Baji and S. Ramakrishna Eds.: Woodhead Publishing, 2021, pp. 147-178.

[3]   A. Šturcová, G. R. Davies and S. J. Eichhorn. "Elastic modulus and stress-transfer properties of tunicate cellulose whiskers". *Biomacromolecules,* Vol. 6, No. 2, pp 1055-1061, 2005.

[4]   J. Tang, J. Sisler, N. Grishkewich and K. C. Tam. "Functionalization of cellulose nanocrystals for advanced applications". *Journal of Colloid and Interface Science,* Vol. 494, pp 397-409, 2017.

[5]   N. Alvarado, J. Romero, A. Torres, C. L. de Dicastillo, A. Rojas, M. J. Galotto and A. Guarda. "Supercritical impregnation of thymol in poly(lactic acid) filled with electrospun poly(vinyl alcohol)-cellulose nanocrystals nanofibers: Development an active food packaging material". *Journal of Food Engineering,* Vol. 217, pp 1-10, 2018.

[6]   J. Heidarbeigi, H. Afshari and A. Borghei. "Study of physical and mechanical properties of pe/cnc nanocomposite for food packaging applications". *Journal of Thermoplastic Composite Materials,* Vol. 34, No. 3, pp 396-408, 2021.

[7]   M. Shakiba, E. Rezvani Ghomi, F. Khosravi, S. Jouybar, A. Bigham, M. Zare, M. Abdouss, R. Moaref and S. Ramakrishna. "Nylon—a material introduction and overview for biomedical applications". *Polymers for Advanced Technologies,* Vol. 32, No. 9, pp 3368-3383, 2021.

[8]   H. Yousefian and D. Rodrigue. "Effect of nanocrystalline cellulose on morphological, thermal, and mechanical properties of nylon 6 composites". *Polymer Composites,* Vol. 37, No. 5, pp 1473-1479, 2016.

[9]   S. K. Rahimi and J. U. Otaigbe. "Polyamide 6 nanocomposites incorporating cellulose nanocrystals prepared by in situ ring-opening polymerization: Viscoelasticity, creep behavior, and melt rheological properties". *Polymer Engineering and Science,* Vol. 56, No. 9, pp 1045-1060, 2016.

[10]   Y. Peng, D. J. Gardner and Y. Han. "Characterization of mechanical and morphological properties of cellulose reinforced polyamide 6 composites". *Cellulose,* Vol. 22, No. 5, pp 3199-3215, 2015.

[11]   J. Shojaeiarani, D. S. Bajwa and N. M. Stark. "Spin-coating: A new approach for improving dispersion of cellulose nanocrystals and mechanical properties of poly (lactic acid) composites". *Carbohydr Polym,* Vol. 190, pp 139-147, 2018.

[12]   D. A. Osorio, E. Niinivaara, N. C. Jankovic, E. C. Demir, A. Benkaddour, V. Jarvis, C. Ayranci, M. T. McDermott, C.-F. de Lannoy and E. D. Cranston. "Cellulose nanocrystals influence polyamide 6 crystal structure, spherulite uniformity, and mechanical performance of nanocomposite films". *ACS Applied Polymer Materials,* Vol. 3, No. 9, pp 4673-4684, 2021.

[13]   A. International, *Astm d882-12, standard test method for tensile properties of thin plastic sheeting*. ASTM International, 2012.

[14]   T. Sucharitpong, N. T. Lam and P. Sukyai. "Production of nylon-6/cellulose nanocrystal composite films using solvent dissolution". *Sugar Tech,* Vol. 22, No. 2, pp 328-339, 2020.

[15]   E. J. Foster, R. J. Moon, U. P. Agarwal, M. J. Bortner, J. Bras, S. Camarero-Espinosa, K. J. Chan, M. J. D. Clift, E. D. Cranston, S. J. Eichhorn, D. M. Fox, W. Y. Hamad, L. Heux, B. Jean, M. Korey, W. Nieh, K. J. Ong, M. S. Reid, S. Renneckar, R. Roberts, J. A. Shatkin, J. Simonsen, K. Stinson-Bagby, N. Wanasekara and J. Youngblood. "Current characterization methods for cellulose nanomaterials". *Chem Soc Rev,* Vol. 47, No. 8, pp 2609-2679, 2018.

[16]   B. Crist and J. M. Schultz. "Polymer spherulites: A critical review". *Progress in Polymer Science,* Vol. 56, pp 1-63, 2016.

[17]   M. García, W. E. van Zyl and H. Verweij. "Hybrid nylon-6/silica nanocomposites with improved mechanical properties". *MRS Online Proceedings Library,* Vol. 740, No. 1, p. I1.9, 2003.

[18]   P. K. Sridhara and F. Vilaseca. "High performance pa 6/cellulose nanocomposites in the interest of industrial scale melt processing". *Polymers,* Vol. 13, No. 9, p. 1495, 2021.

[19]   S. Aitha and N. Vasanthan. "Effect of cellulose nanocrystals on crystallization, morphology and phase transition of polyamide 6". *Composite Interfaces,* Vol. 27, No. 4, pp 371-384, 2020.

[20]   J. Pagacz, K. N. Raftopoulos, A. Leszczyńska and K. Pielichowski. "Bio-polyamides based on renewable raw materials". *Journal of Thermal Analysis and Calorimetry,* Vol. 123, No. 2, pp 1225-1237, 2016.

[21]   K.-H. Lee, K.-W. Kim, A. Pesapane, H.-Y. Kim and J. F. Rabolt. "Polarized ft-ir study of macroscopically oriented electrospun nylon-6 nanofibers". *Macromolecules,* Vol. 41, No. 4, pp 1494-1498, 2008.

[22]   N. Vasanthan and D. R. Salem. "Ftir spectroscopic characterization of structural changes in polyamide-6 fibers during annealing and drawing". *Journal of Polymer Science Part B: Polymer Physics,* Vol. 39, No. 5, pp 536-547, 2001.

[23]   Y. Li and W. A. Goddard. "Nylon 6 crystal structures, folds, and lamellae from theory". *Macromolecules,* Vol. 35, No. 22, pp 8440-8455, 2002.

[24]   E. Klata, S. Borysiak, K. Van de Velde, J. Garbarczyk and I. Krucinska. "Crystallinity of polyamide-6 matrix in glass fibre/polyamide-6 composites manufactured from hybrid yarns". *Fibres & Textiles in Eastern Europe,* Vol. 12, No. 3, pp 64-69, 2004.

[25]   M. S. Reid, M. Villalobos and E. D. Cranston. "Benchmarking cellulose nanocrystals: From the laboratory to industrial production". *Langmuir,* Vol. 33, No. 7, pp 1583-1598, 2017.

[26]   Z. M. Huang, Y. Z. Zhang, M. Kotaki and S. Ramakrishna. "A review on polymer nanofibers by electrospinning and their applications in nanocomposites". *Composites Science and Technology,* Vol. 63, No. 15, pp 2223-2253, 2003.

[27]   J. Xue, T. Wu, Y. Dai and Y. Xia. "Electrospinning and electrospun nanofibers: Methods, materials, and applications". *Chemical Reviews,* Vol. 119, No. 8, pp 5298-5415, 2019.

[28]   M. B. Bazbouz and G. K. Stylios. "Alignment and optimization of nylon 6 nanofibers by electrospinning". *Journal of Applied Polymer Science,* Vol. 107, No. 5, pp 3023-3032, 2008.

[29]   A. Awal, M. Sain and M. Chowdhury. "Preparation of cellulose-based nano-composite fibers by electrospinning and understanding the effect of processing parameters". *Composites Part B-Engineering,* Vol. 42, No. 5, pp 1220-1225, 2011.

[30]   J. I. Kim, T. I. Hwang, L. E. Aguilar, C. H. Park and C. S. Kim. "A controlled design of aligned and random nanofibers for 3d bi-functionalized nerve conduits fabricated via a novel electrospinning set-up". *Scientific Reports,* Vol. 6, No. 1, p. 23761, 2016.

[31]   M. S. Islam, J. R. McCutcheon and M. S. Rahaman. "A high flux polyvinyl acetate-coated electrospun nylon 6/sio2 composite microfiltration membrane for the separation of oil-in-water emulsion with improved antifouling performance". *Journal of Membrane Science,* Vol. 537, pp 297-309, 2017.